

PAPER

Performance analysis of LEO augmented GNSS precise point positioning from in-orbit CENTISPACE™ satellites

To cite this article: Weiguang Gao *et al* 2025 *Meas. Sci. Technol.* **36** 016338

View the [article online](#) for updates and enhancements.

You may also like

- [Advanced detection methods for tunnels and roadways: a review](#)
Dingchao Chen, Xiangyu Wang, Jianbiao Bai *et al.*
- [Multi-objective tree-structured Parzen estimator optimized Res-Net for ITSC fault diagnosis of PMSM](#)
Wei Zhang, Qiwei Xu, Yixuan Zhang *et al.*
- [An adaptive acoustic signal reconstruction and fault diagnosis method for rolling bearings based on SSDAE-MobileViT](#)
Yingkui Gu, Puzhou Wang, Yin Li *et al.*

The advertisement features the ECS logo and the text "The Electrochemical Society Advancing solid state & electrochemical science & technology". On the left, there's a circular logo for "SUSTAINABLE TECHNOLOGIES" with a stylized globe and leaves. Below it, the text reads: "249th ECS Meeting May 24-28, 2026 Seattle, WA, US Washington State Convention Center". On the right, the main headline is "Spotlight Your Science" with a "Submission deadline: December 5, 2025" below it. A green button at the bottom right says "SUBMIT YOUR ABSTRACT".

Performance analysis of LEO augmented GNSS precise point positioning from in-orbit CENTISPACE™ satellites

Weiguang Gao^{1,3}, Xin Xie^{2,*}, Yinan Meng^{1,3}, Qiang Li², Hanlin Chen², Long Yang⁴, Tao Geng² and Qile Zhao²

¹ Beijing Institute of Tracking and Telecommunication Technology, Beijing, People's Republic of China

² GNSS Research Center, Wuhan University, 129 Luoyu Road, Wuhan 430079, People's Republic of China

³ Key Laboratory of Smart Earth, Beijing, People's Republic of China

⁴ Beijing Future Navigation Tech Co., Ltd, No. 81 Beiqing Road, Beijing 100081, People's Republic of China

E-mail: xiexin@whu.edu.cn

Received 3 August 2024, revised 11 November 2024

Accepted for publication 29 November 2024

Published 19 December 2024



Abstract

Low Earth orbit (LEO) satellites can be used to augment global navigation satellite system (GNSS) precise point positioning (PPP) for rapid convergence, which has been demonstrated by an abundance of simulation studies. In this contribution, we analyze the performance of LEO augmented GNSS PPP using real data from two in-orbit CENTISPACE™ experimental satellites launched by Beijing Future Navigation Tech Co., Ltd. The onboard GNSS observations are used to determine the precise orbits and the initial clock offsets of LEO satellites, and the clock corrections are estimated using the observations from a ground network. The RMS values of measurement residuals for dual-frequency ionosphere-free combination of LEO downlink pseudorange and phase observations are about 0.8 m and 2 cm. We select three ground tracking stations for the PPP experiment and the performance of GPS, BeiDou Navigation Satellite System (BDS)-3, GPS + BDS-3, GPS + BDS-3 + Galileo PPP with the augmentation of 1 and 2 LEO satellites is evaluated and analyzed. The results indicate that the observations from LEO satellites can significantly improve the GNSS convergence performance. Compared with GNSS-only PPP, the convergence time is shortened by more than 50% with the addition of 1 LEO satellite, while the two LEO satellites achieve an improvement of 68%–73%. In particular, to achieve a horizontal accuracy of better than 10 cm, the convergence time for the GPS + BDS-3 + Galileo PPP solutions is reduced from 10.8 min to 3–5 min with the augmentation of 1–2 LEO satellites, which reveals the excellent potential of LEO satellites for rapid PPP convergence. The correlation analysis between ambiguity parameters and other related parameters during the PPP processing also demonstrates the superior performance of the LEO satellites in accelerating the PPP convergence. Furthermore, the GNSS/LEO combined PPP improves the 3D positioning accuracy by 10%–20%.

* Author to whom any correspondence should be addressed.

Keywords: LEO navigation augmentation, precise point positioning, rapid convergence, CENTISPACETM satellites, GNSS

1. Introduction

With the continuous expansion and refinement of satellite navigation applications, real-time high-precision positioning services in wide areas are becoming an important development trend of global navigation satellite systems (GNSSs). The high-precision and global availability of precise point positioning (PPP) technology make it very promising and a research hotspot [1, 2]. However, the long convergence time of PPP is unacceptable for time-critical scenarios. Therefore, many efforts have been made to break this constraint, such as PPP ambiguity resolution and PPP-real-time kinematic (PPP-RTK) methods [3–6]. Although the PPP-RTK method can significantly shorten the initialization time to obtain fast positioning results with high precision, this technology can only provide regional service and requires a dense network of reference stations. As a consequence, global high-precision positioning with rapid convergence remains a major challenge in the GNSS community.

In recent years, a notable shift in investments of the space industry has occurred, moving away from medium and high Earth orbit satellite constellations and applications toward those centered on low Earth orbit (LEO) satellites. The rapid growth in the number of LEO satellites opens up the possibility of providing a PNT service [7, 8]. Compared with classical GNSS medium Earth orbit (MEO) satellites, LEO satellites, being closer to Earth, can provide stronger navigation signals, which makes them more resilient to jamming [9, 10]. Moreover, the faster geometry changes from fast-moving LEO satellites result in a quicker decorrelation of parameters, ultimately speeding the PPP convergence [11]. Thus, bringing LEO constellations into the GNSS system creates the opportunity for global, reliable, rapid, high-precision positioning. Given these benefits, the concept of LEO augmented GNSS PNT has emerged and attracted extensive attention. In China, the LEO constellation stands as a crucial point in the advancement of the next-generation BeiDou Navigation Satellite System (BDS) and has been taken into a national comprehensive PNT system [12, 13]. Europe is stepping forward with LEO-PNT plans with a small constellation of LEO demonstration satellites [14], which will demonstrate the benefits of working in combination with Galileo and other GNSSs in a multi-layer approach.

To explore how to effectively implement the forthcoming LEO-augmented PNT, many simulations have been conducted, focusing on constellation optimization [15], signal structure and frequency design [16, 17], precise orbit and clock determination [18, 19], atmospheric models [20, 21], broadcast ephemeris models [22, 23], and positioning performance analysis [19, 24]. Among these simulation studies, the demonstration of LEO augmented high-precision positioning with

dedicated signals has been a research focus and hotspot in recent years. Ge *et al* [25] explored the potential of LEO enhanced GNSS (LeGNSS) PPP based on the simulated observations of BDS, GPS, and Iridium satellite constellation with 66 LEO satellites. They confirmed that the combination of the Iridium constellation can shorten the convergence time of GPS + BDS PPP from about 30 min to 5 min in most of the areas of the world. In the simulation of Li *et al* [19], the convergence time for GPS + BDS + GLONASS + BDS PPP can be significantly reduced from about 10 min to 1–3 min by integrating LEO constellations with about 200–300 satellites. Ge *et al* [15] also explored the LEO constellation optimization for LeGNSS and promoted the idea of combination of several LEO constellations with different inclinations to improve the global service performance. Through the simulations involving 120–240 LEO satellites with orbital inclinations varying from 35°–90°, the convergence time of LeGNSS PPP can be reduced to less than 1 min with the deployment of suitable LEO constellations. Gao *et al* [26] simulated a LEO constellation with 120 satellites at 55° inclination and 30 satellites at 89° inclination to enhance the performance of the BDS. The positioning results indicate that PPP convergence time is shortened by about 20 times to 1 min with a 10 cm threshold when LEO constellations are integrated into BDS.

By recognizing the importance of LEO navigation augmentation and demonstrating its significant potential, some commercial aerospace industries have also begun to develop LEO navigation augmentation systems. In the United States, the Xona Space System initiated the ‘PULSAR’ project with a LEO constellation of between 250 and 300 small satellites for powerful, precise, protected LEO-PNT service [27]. Several demonstration satellites have been launched to validate the capability of its patented core PULSAR technology, such as precise LEO PNT signals transmission and distributed clock architecture. However, no specific verification results have been released. The Luojia-1A scientific experimental satellite launched in June 2018 and developed by Wuhan University has the ability of LEO navigation signal augmentation. Initial assessments reveal that the accuracies of pseudorange and carrier phase from Luojia-1A navigation augmentation signals are about 0.8 m and 2.8 mm, respectively [28]. However, the performance of PPP enhanced by the Luojia-1A satellite has not been reported yet. Following this, Chinese space companies launched several experimental satellites with the function of navigation augmentation, including projects such as ‘Hongyan’, ‘Hongyun’, and ‘WT01’ [29, 30]. The China Satellite Network Group Co., Ltd has begun building a LEO communication constellation with navigation augmentation capability. In addition, a dedicated LEO navigation augmentation system, named ‘CENTISPACETM’, has been proposed and developed by Beijing Future Navigation Tech Co.,

Ltd. Five CENTISPACE™ experimental satellites have been successfully deployed since its first launch in 2018, which provides a valuable opportunity for investigating the contribution of LEO satellites to GNSS PPP. Li *et al* [31] and Xu *et al* [32] preliminarily carried out the GNSS and LEO combined PPP based on 1 and 2 CENTISPACE™ experimental satellites, respectively. The results show that the GNSS PPP convergence time can be shortened by about 20%–50% with the inclusion of CENTISPACE™ LEO satellites.

In this study, real tracking data from two CENTISPACE™ experimental satellites are used to assess LEO augmented GNSS PPP performance, especially for the convergence time. This follows the introduction of the CENTISPACE™ LEO constellation and ground-tracking data. The observation characteristics of LEO downlink navigation signals from CENTISPACE™ experimental satellites are analyzed and the data processing strategies of GNSS and LEO combined PPP is presented. In particular, this paper also provides a detailed description of the orbit and clock offset determination strategies and results of the CENTISPACE™ satellites. Afterwards, the GNSS/LEO combined PPP results are shown and the LEO-augmented PPP performance is assessed. Potential mechanisms for accelerating convergence are explored by analyzing variations in the correlation between ambiguity and other parameters to be estimated. Finally, the conclusions and future work are given.

2. Data collection

2.1. CENTISPACE™ satellites

CENTISPACE™ is a commercial LEO navigation augmentation system designed by Chinese Beijing Future Navigation Tech Co., Ltd. This system will be built to provide global high-precision positioning augmentation and GNSS integrity monitoring services [33]. As early as September 2018, Beijing Future Navigation Tech Co., Ltd. launched the first CENTISPACE™ experimental satellite. The preliminary signal verification of LEO navigation augmentation has been completed. From September to December in 2022, four CENTISPACE™ experimental satellites were launched to conduct further key technology validation [34]. LEO downlink navigation signal quality and LEO precise positioning augmentation performance is included in major validation missions.

In contrast to typical LEO satellites, the CENTISPACE™ satellites not only receive signals from current GNSS satellites, but also simultaneously transmit navigation augmentation signals. For compatibility and interoperability with existing GNSS systems, the CENTISPACE™ experimental satellites broadcast signals at CL1 and CL5 frequencies centered at 1575.42 and 1176.45 MHz, as detailed by Yang [33]. The CENTISPACE™ navigation signals use code division multiple access model and binary phased-shift keying modulation. The chip rates are 2.046 Mcps [33, 34].

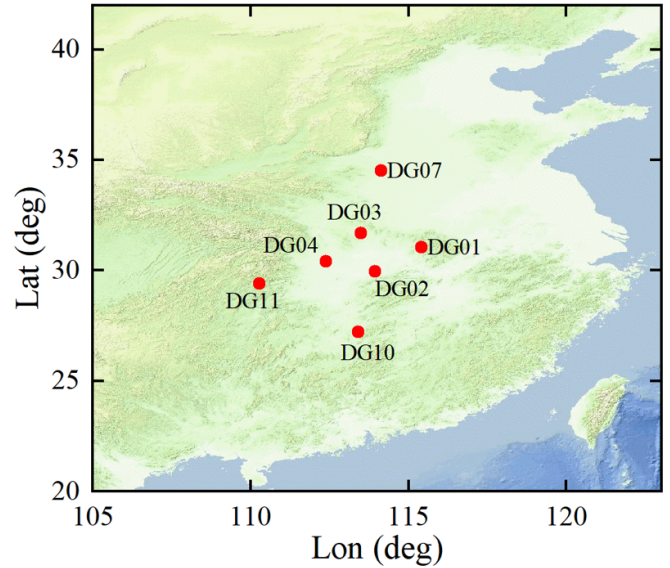


Figure 1. Distribution of the selected ground stations capable of tracking GNSS and CENTISPACE™ satellites.

In addition, the experimental satellite is equipped with an onboard GNSS receiver with the capacity of tracking BDS-3 B1C/B2a/B3I, GPS L1/L2/L5, and Galileo E1/E5a signals. The primary contribution of onboard GNSS observations is to conduct the precise orbit determination (POD) of the CENTISPACE™ satellite. Meanwhile, the GNSS receivers onboard CENTISPACE™ satellites are engineered to enhance BDS-3 POD and global integrity monitoring.

2.2. Ground tracking stations

Along with the construction of CENTISPACE™ space constellation, ground tracking stations have been established to track, monitor, and assess the signals of CENTISPACE™ satellites. Beijing Future Navigation Tech Co., Ltd. provides dedicated receiving equipment and jointly builds a number of monitoring stations for tracking CENTISPACE™ experimental satellites with the GNSS Research Center of Wuhan University, which is authorized to analyze and study the data obtained from these monitoring stations. In this study, a regional network consisting of seven stations located in southern China is selected for analysis, as shown in figure 1. The raw data used in this paper are all sourced from these monitoring stations and authorized by Beijing Future Navigation Tech Co., Ltd. These stations can simultaneously receive GPS L1/L2/L5, BDS-2 B1I/B2I/B3I, BDS-3 B1I/B3I/B1C/B2a, Galileo E1/E5a/E5b, and CENTISPACE™ CL1/CL5 signals. The GPS/BDS/Galileo and CENTISPACE™ observations from these tracking stations were collected from June 27 to June 30, 2023. During this period, two CENTISPACE™ satellites (named ESAT1 and ESAT2 in this paper by Beijing Future Navigation Tech Co., Ltd), are simultaneously tracked by these stations.

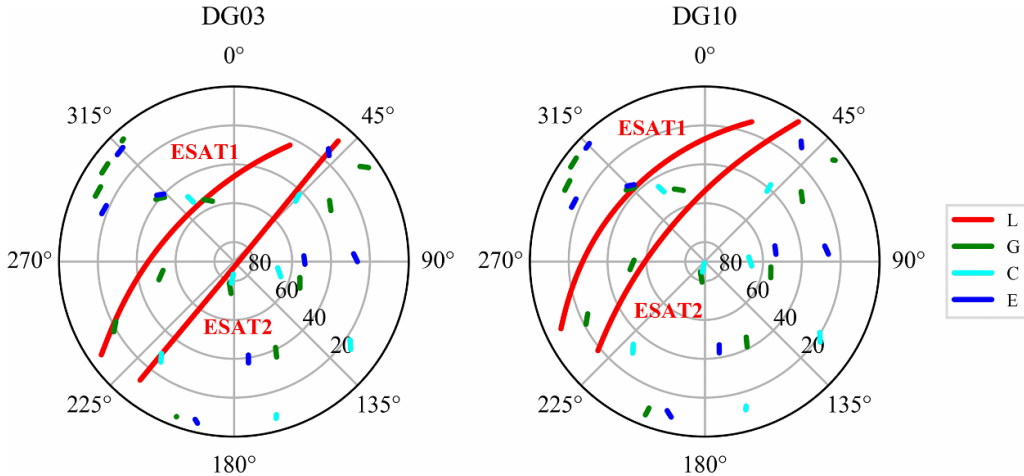


Figure 2. Sky plots (azimuth vs elevation) of GPS (G), BDS-3 (C), Galileo (E) and two LEO (L) satellites during 10 min at the stations DG03 (left) and DG10 (right).

2.3. Tracking characteristics of LEO navigation observations

In previous simulation studies, the sky plots of the GNSS and LEO satellites were usually analyzed and compared to show rapid geometric changes of the LEO satellites over stations. In this study, real observations of ground stations tracking the GNSS and LEO satellites are used to depict satellite sky-view tracks. Figure 2 shows the sky plots of BDS-3, GPS, Galileo satellites and two CENTISPACE™ experimental satellites (ESAT1 and ESAT2) during a 10 min of observation length for the stations DG03 and DG10. The orbits of CENTISPACE™ experimental satellites are at an altitude of roughly 700 km and an inclination angle of about 54°, leading to a pass duration of around 10 min for ground stations, which is greatly shorter than that of GNSS satellites. As depicted in figure 2, it is evident that the tracks of ESAT1 and ESAT2 satellites extend much longer than those of GNSS satellites over the same ten-minute interval. This fast variation in geometry plays a crucial role in PPP convergence. The two CENTISPACE™ satellites distinctly exhibit a rise and set pattern in the sky plots, while the GNSS satellites display incomplete tracking arcs. For the station DG03, the elevation angle of the ESAT2 satellite increases from around 5° to 90° and then decreases to about 5°, while the elevation angle of the ESAT1 satellite varies only from around 5° to 55°. For the station DG10, the elevation angles of the ESAT1 and ESAT2 satellite vary about 5°–40° and 2°–65°, respectively. The tracking trajectory of the ESAT2 satellite is slightly longer than that of the ESAT1 satellite for both stations.

3. Data processing

3.1. LEO augmented PPP model

For PPP, the well-known dual-frequency ionosphere-free (IF) combination is used to eliminate the ionosphere effect. The observation model of IF code and carrier phase combination (PC and LC) can be expressed as:

$$\begin{aligned} P_r^{S,k} &= \rho_r^{S,k} + c(\text{dt}_r^S - \text{dt}^{S,k}) + m^{S,k}T_r + \varepsilon_P^{S,k} \\ L_r^{S,k} &= \rho_r^{S,k} + c(\text{dt}_r^S - \text{dt}^{S,k}) + m^{S,k}T_r + \lambda^S N_r^{S,k} + \varepsilon_L^{S,k} \end{aligned} \quad (1)$$

where the superscripts S , k and r denote the GNSS system, the satellite and the station, respectively; P and L are the IF code and carrier phase combination, respectively; ρ is the geometry distance between the receiver and GNSS satellite; c denotes the propagation speed of light in a vacuum; dt_r^S is the receiver clock offset associated with the GNSS system; $\text{dt}^{S,k}$ denotes satellite clock offset; T_r and $m^{S,k}$ denote the zenith tropospheric delay (ZTD) and its mapping function, respectively; λ and N are the wavelength and ambiguity of the IF combination, respectively; ε_P and ε_L denote combined error of multipath effect and measurement noise of IF code and carrier phase combination, respectively. It is worth noting that correction terms such as relativistic effects, antenna phase centers, and phase windup, have been omitted from equation (1) to simplify the expression.

In the LEO augmented PPP, the LEO satellite observations are processed together with GNSS satellite observations. The LEO system can be regarded as a unique GNSS system, thus the IF code and carrier phase combination observation model for multi-GNSS and LEO satellites can be written as follows,

$$\begin{aligned} P_r^{S,k} &= \rho_r^{S,k} + c(\text{dt}_r^G + b_r^S - \text{dt}^{S,k}) + m^{S,k}T_r + \varepsilon_P^{S,k} \\ L_r^{S,k} &= \rho_r^{S,k} + c(\text{dt}_r^G + b_r^S - \text{dt}^{S,k}) + m^{S,k}T_r + \lambda^S N_r^{S,k} + \varepsilon_L^{S,k} \\ P_r^{L,k} &= \rho_r^{L,k} + c(\text{dt}_r^G + b_r^L - \text{dt}^{L,k}) + m^{L,k}T_r + \varepsilon_P^{L,k} \\ L_r^{L,k} &= \rho_r^{L,k} + c(\text{dt}_r^G + b_r^L - \text{dt}^{L,k}) + m^{L,k}T_r + \lambda^L N_r^{L,k} + \varepsilon_L^{L,k} \end{aligned} \quad (2)$$

where the superscript G stands for the GPS which is selected here as the reference system, and L represents the LEO system; b_r^S is the receiver inter-system bias (ISB) between the GNSS system S and the reference system, and its value is 0 when $S = G$; Likewise, b_r^L denotes the ISB between the LEO system and the reference system.

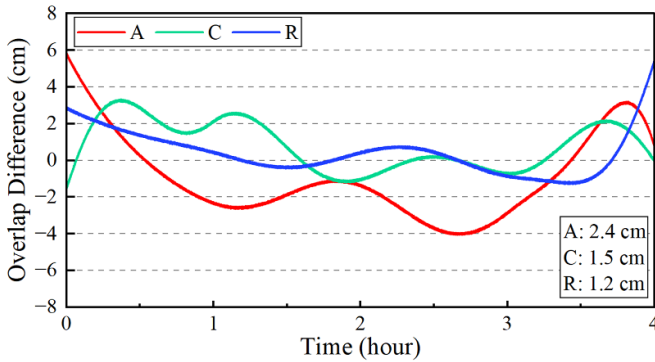


Figure 3. Orbit overlap differences in the along-track (A), cross-track (C) and radial (R) components for the GNSS-based orbit solutions of the ESAT2 satellite.

3.2. Data processing strategy

To conduct LEO-augmented GNSS PPP, precise orbits and clock offsets for both GNSS and LEO satellites are required. For GNSS satellites, the Wuhan University analysis center (WUM) final precise products from the International GNSS Service multi-GNSS Pilot Project (IGS MGEX) are used. The accuracy of WUM final orbits and clocks for GPS, Galileo and BDS-3 is better than 10 cm and 0.1 ns [35]. For the CENTISPACE™ satellites, their precise orbits and onboard clock offsets are generated using onboard GNSS-based LEO POD method, and are provided by Beijing Future Navigation Tech Co., Ltd taking ESAT2 satellite as an example, the orbit overlap differences from GNSS-based POD results are shown in figure 3. In this study, the LEO orbit determination arc is 28 h, and a 4 h orbit overlap comparison between consecutive arcs is used. The RMS values of orbit overlap comparison in along-track, cross-track and radial components for the ESAT2 satellite are 2.4 cm, 1.5 cm and 1.2 cm, respectively, which can meet the needs of the LEO-augmented GNSS PPP validation.

Although the onboard GNSS receiver and downlink navigation signals share the same atomic clock for the CENTISPACE™ experimental satellites, the time when the LEO onboard receiver receives GNSS signals is inconsistent with the time when the LEO satellite broadcasting downlink navigation signals, and there is a time offset between receiving and broadcasting signals for the LEO satellite. Therefore, the LEO onboard receiver clock offsets determined by the aforementioned GNSS-based LEO POD processing cannot be directly used for PPP, and a time synchronization processing needs to be carried out. In this study, we redetermine LEO satellite clock offsets at the transmitter based on LEO downlink pseudorange and carrier-phase measurements from the ground tracking network shown in figure 1. During LEO satellite clock estimation, the initial values are set to GNSS-based LEO onboard receiver clock offsets and the satellite orbits are fixed to the GNSS-based orbit solutions. The measurement residuals of seven ground stations for dual-frequency IF combination of CL1/CL5 pseudorange (PC) and phase (LC) observations from LEO satellite clock estimation are displayed in figure 4. The PC and LC measurement residuals present

variations within ± 4 m and ± 10 cm for both ESAT1 and ESAT2 satellites at these stations. We observe that the residuals are more pronounced at the start and end of the time series, which is attributed to the lower elevation angles. The RMS values of measurement residuals for LC and PC observations from two CENTISPACE™ experimental satellites are about 2 cm and 0.8 m.

After obtaining precise orbits and clock offsets for GNSS and LEO satellites, the GNSS and LEO combined PPP are carried out. The detailed processing strategy is summarized in table 1. Using real multi-GNSS and LEO observations from ground stations, the LEO-augmented single or multi-GNSS PPP performance is analyzed in this paper. Dual-frequency ionospheric-free combinations of BDS-3 B1I/B3I, GPS L1/L2, Galileo E1/E5a and CENTISPACE™ CL1/CL5 pseudorange and carrier-phase measurements are used. In PPP processing, the sampling interval is 1 s, and the *a priori* sigma of raw pseudorange and carrier phase measurements are respectively 1 m and 1 cm for all systems. An elevation mask of 7° is set for valid measurements, and an elevation-dependent weighting strategy is employed. During the measurement modeling process, the antenna phase center corrections from the igs20.atx file are utilized for the multi-GNSS satellites, and manufacturer-provided phase center offset (PCO) values are applied for CENTISPACE™ LEO satellites with no phase center variation (PCV) available. Additional corrections for other errors such as station tidal displacements, relativistic effects, and phase wind-up are made based on existing models. A sequential filtering approach is employed to estimate the station coordinates, ZTDs, receiver clock offsets, and float ambiguity parameters. In addition, the ISB parameters are estimated as constants for the multi-GNSS or GNSS/LEO combined PPP solutions.

4. LEO augmented GNSS PPP analysis

4.1. PPP error time series

Using real observational data from the GNSS and CENTISPACE™ experimental satellites, the LEO-augmented GNSS PPP performance is analyzed. Three stations (DG03, DG10, DG11) with superior data quality are selected for the simulated kinematic PPP analysis. The daily static PPP solutions from the stations serve as the reference coordinates for calculating the PPP positioning errors. In this study, the PPP convergence condition requires that the horizontal positional error decreases to and stays below 0.1 m, and the vertical error decreases to and remains below 0.2 m for a continuous duration of at least 5 min (300 epochs). We then analyze the differences in the positioning results before and after the combination of one or two LEO satellites to investigate the effect of LEO-augmented GNSS PPP. Due to the short tracking time of LEO satellites, the arc length of data processing is 1 h in this study, and the LEO satellites are only involved in PPP processing for approximately ten minutes at the beginning of the period.

The one-hour data during 13:50:00–14:50:00 on DOY 180, 2023, is selected as an example for analysis. The

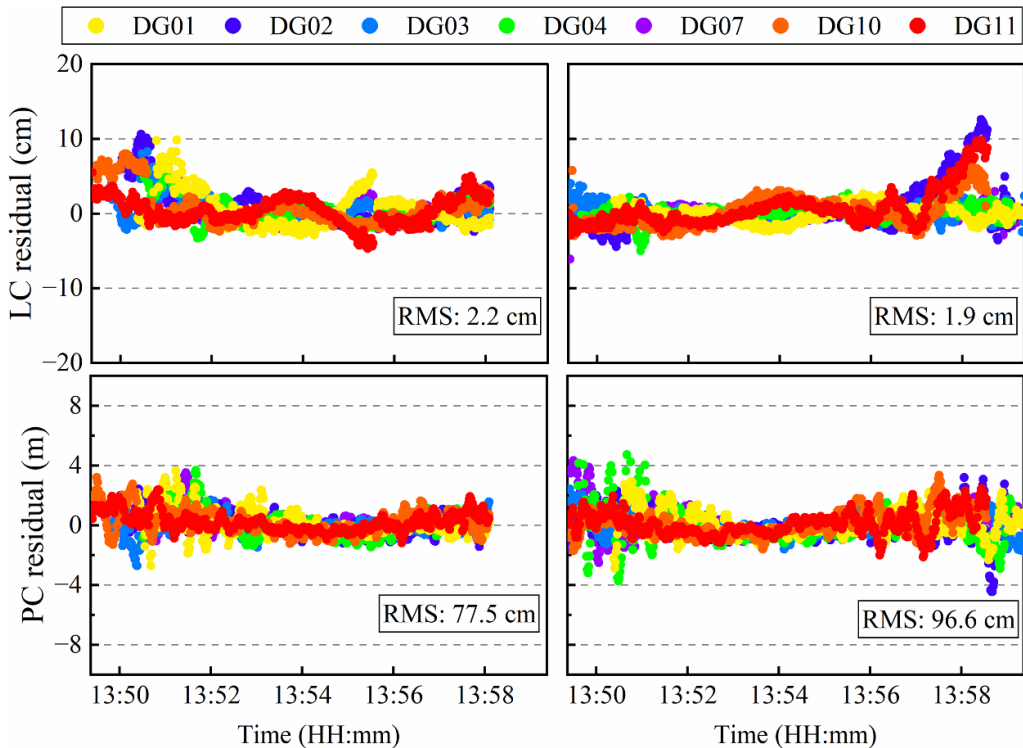


Figure 4. LC and PC measurement residuals of 7 ground stations for the ESAT1 (left) and ESAT2 (right) satellites.

Table 1. GNSS/LEO combined PPP processing strategies.

Items	Description
Constellations	BDS-3, GPS, Galileo, CENTISPACE™ ESAT1 and ESAT2 satellites
Signals	BDS-3: B1I/B3I, GPS: L1/L2, Galileo: E1/E5a, CENTISPACE™: CL1/CL5
Modeled observable	Dual-frequency ionosphere-free combination
Sampling interval	1 s
Cut-off elevation	7°
<i>A priori</i> observation noise	Pseudorange: 1.0 m; carrier-phase: 1.0 cm
Weighting	Elevation-dependent weighting strategy
GNSS orbit and clock	WUM final products [35]
LEO orbit and clock	Orbit: POD solutions using onboard GNSS observations Clock: Estimated using ground tracking observations
Ionospheric delay	First-order eliminated with ionosphere-free combination
Tropospheric delay	GPT2w model for meteorological parameters, Saastamoinen model [36] for <i>a priori</i> delays with the Global Mapping Function [37]; residual wet delays estimated as a random walk process
Satellite PCO/PCV	GNSS: Corrected by igs20.atx for PCO and PCV LEO: PCO values from the manufacturer and PCV neglected
Inter-system bias	Estimated as a constant
Phase windup	Corrected by model [38]
Tidal displacement	Corrected according to IERS 2010 [39]
Ambiguity	Estimated as a float constant within an arc without cycle slips
Station Position	White noise
Receiver clock offset	White noise

number of visible satellites for GPS, BDS-3, Galileo, and CENTISPACE™ constellations during one hour at stations DG03 and DG10 is shown in figure 5. The number of satellites for the GPS, BDS-3, and Galileo constellations falls within the ranges of 11–13, 11–12, and 7–9, respectively. For the CENTISPACE™ LEO satellites, these stations begin to

receive navigation signals from ESAT1 and ESAT2 satellites at about 13:50:00. The ESAT1 and ESAT2 satellites could be observed simultaneously for about 8 min after the start, while only the signals from ESAT2 could be received for a period of about 8–10 min. After that, both stations will not be able to track the signals from the CENTISPACE™ satellites until

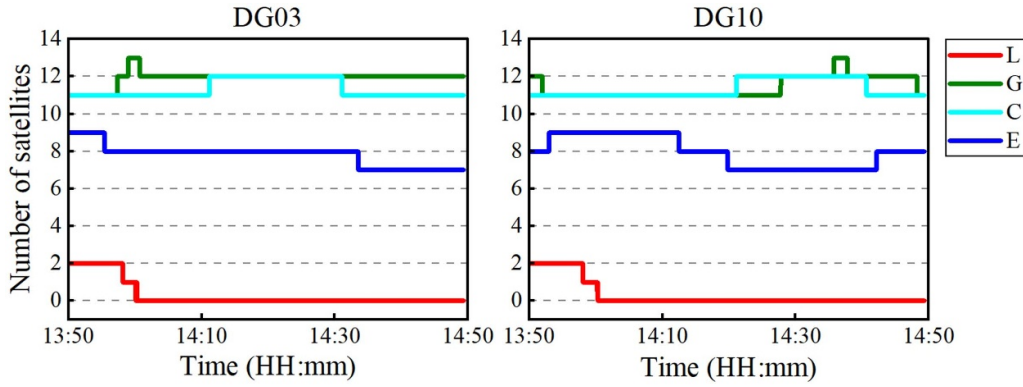


Figure 5. Number of GNSS and LEO satellites tracked at stations DG03 (left) and DG10 (right) during 13:50:00–14:50:00, DOY 180, 2023.

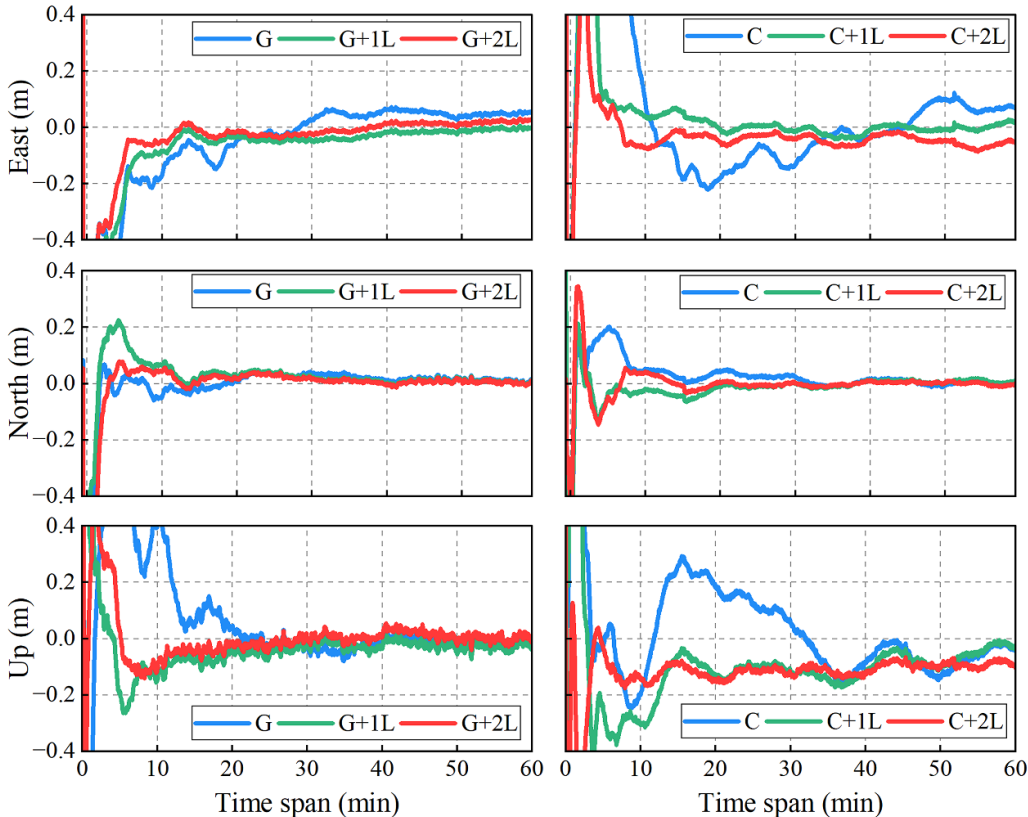


Figure 6. Positioning error time series in the east, north, and up directions for one and two LEO satellites augmented GPS (left) and BDS-3 (right) PPP solutions at the station DG10.

the next orbital period, as the two LEO satellites have already passed through the territory.

For the LEO-augmented GNSS PPP analysis, the concerned GNSS constellation schemes in this study include GPS (G), BDS-3 (C), GPS/BDS-3 (GC), and GPS/BDS-3/Galileo (GCE). Following this, one (ESAT2) and two LEO satellites (ESAT1 and ESAT2) are combined and processed using the same approach, resulting in a total of 12 kinematic PPP solutions. The decision to include the ESAT2 satellite rather than the ESAT1 in the GNSS + 1LEO scheme is due to its longer observable time during the study period.

Taking station DG10 as a case in point, figure 6 shows the positioning error series of GPS (G) and BDS-3 (C) PPP solutions with and without the augmentation of LEO satellites. As shown in the figure, the PPP can converge in a shorter time after including two LEO satellites, and the positioning errors are more stable after convergence in the east (E), north (N), and up (U) directions. In addition, an obvious improvement can be observed for positioning error series in the east and up directions, while the impact is relatively slight in the north direction. For a single-system GPS or BDS-3 PPP solution, adding one LEO satellite reduces the convergence time from

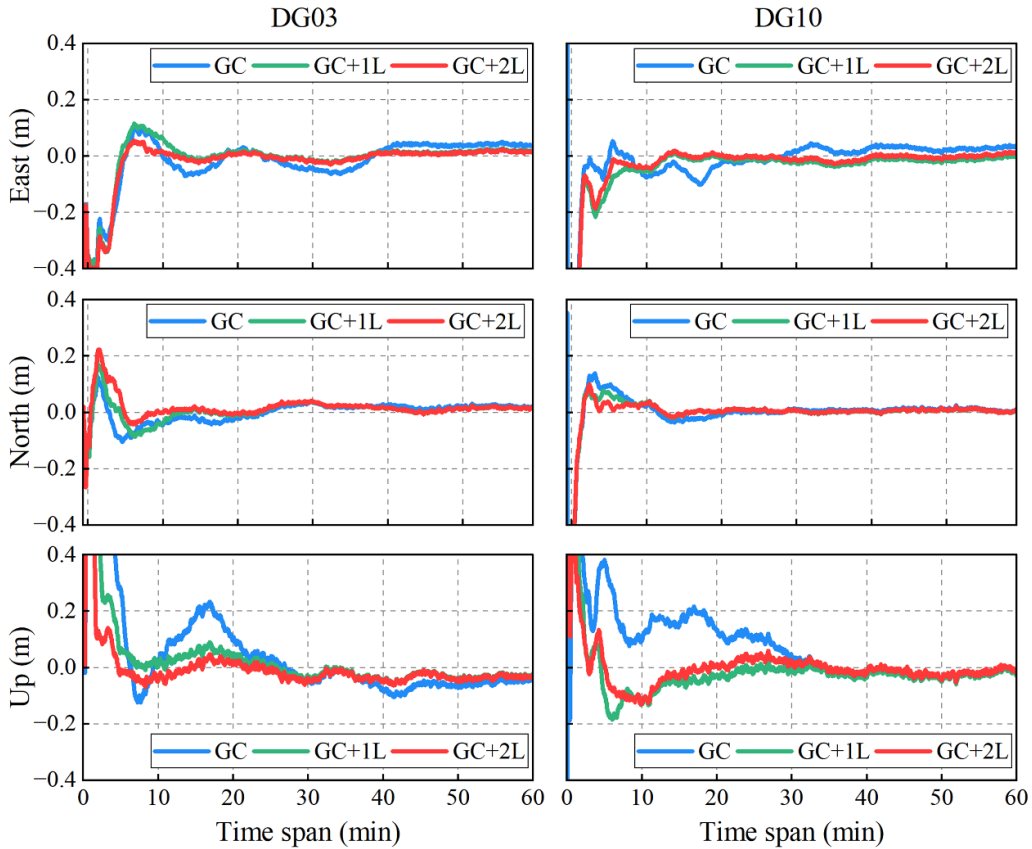


Figure 7. Positioning error time series for one and two LEO satellites augmented GPS + BDS-3 PPP solutions at stations DG03 (left) and DG10 (right).

about 20–30 min to 7–9 min in the east component, while the convergence time is further shortened to 4–6 min with the combination of two LEO satellites. In the up component, the positioning convergence time is reduced from about 12–20 min to 7–11 min, and 3–4 min with the introduction of one and two LEO satellites, respectively. It should be noted that the PPP convergence condition for the east direction is 10 cm, while it is 20 cm for the up direction. The addition of LEO satellites effectively speeds up GPS and BDS-3 PPP convergence, especially in the east and up directions, demonstrating the positive impact of LEO satellites on PPP performance.

The effects of LEO satellites on GPS + BDS-3 (GC) and GPS + BDS-3 + Galileo (GCE) PPP are further compared and analyzed. The positioning error time series of LEO augmented GPS + BDS-3 PPP solution at stations DG03 and DG10 is shown in figure 7, and the results of LEO augmented GPS + BDS-3 + Galileo PPP solution are displayed in figure 8. From the figures, it is evident that the inclusion of LEO satellites significantly improves the positioning stability and convergence speed, especially in the up direction. The results show that introducing 2 LEO satellites has a better effect than that of 1 LEO satellite. For the GC PPP solution, the convergence time of the PPP errors smaller than 20 cm in the up direction is reduced from about 18 min to 2–3 min after introducing 1–2 LEO satellites, demonstrating a remarkable effect. Additionally, GCE + 1L and GCE + 2L also reduce

the convergence time of the up direction from about 7 min to 1–2 min. This indicates that LEO satellites have a very inspiring enhancement effect on multi-GNSS PPP performance.

4.2. PPP convergence time and accuracy analysis

The statistical results of PPP convergence times for three stations are computed and shown in figure 9. As presented in figure 10, the addition of LEO satellites dramatically accelerates the PPP convergence speed, regardless of whether it is the single- or multi-GNSS PPP solution. Furthermore, the addition of 2 LEO satellites can further enhance this effect. For instance, at the DG11 station, the PPP convergence times for G, C, GC, and GCE solutions are 24.6, 28.8, 13.0, and 9.8 min, respectively. After adding one LEO satellite, these times are reduced to 8.2, 11.6, 7.8, and 4.4 min, and further reduced to 7.9, 7.8, 4.1, and 3.5 min after adding two satellites.

The average convergence times of the three stations for each PPP solution are listed in table 2. Analysis of the results reveals that when using only GNSS, both G and C take more than 20 min to achieve convergence. However, utilizing GC and GCE reduces this process to 16.22 and 10.8 min respectively, demonstrating that employing more GNSS systems can expedite PPP convergence. Furthermore, the inclusion of LEO satellites in the GNSS + LEO solution significantly enhances convergence speed. Notably, in the case of C + 1L, the convergence speed surpasses that of the GC scheme, while the

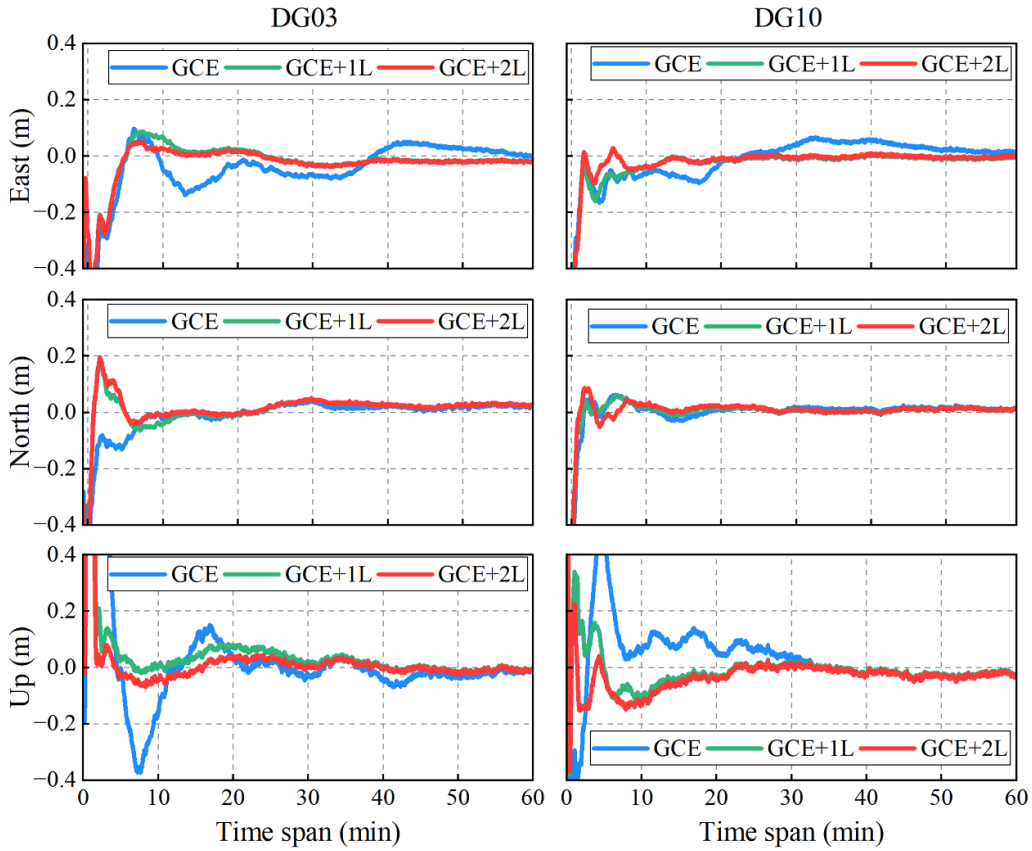


Figure 8. Positioning error time series for one and two LEO satellites augmented GPS + BDS-3 + Galileo PPP solutions at stations DG03 (left) and DG10 (right).

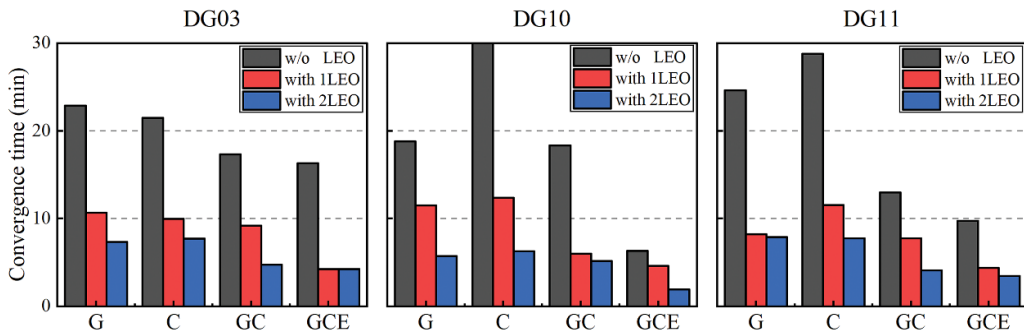


Figure 9. Convergence times of each GNSS PPP solution without LEO, with 1 and 2 LEO satellites at stations DG03, DG10 and DG11.

G + 1L solution even outperforms the GCE solution. In particular, the combination of 1 and 2 LEO satellites for G and C PPP solutions can decrease the averaged convergence time from 24.7 min to within 12 and 8 min. For the GC solution, the convergence time can be reduced from 16.2 min to within 8 and 5 min with 1 and 2 LEO satellites, respectively. Similarly, for the GCE solution, it can be shortened from 10.8 min to 3–5 min. Overall, compared to the GNSS-only PPP, the addition of 1 LEO satellite can reduce the convergence time by more than 50%, while adding 2 LEO satellites can lead to a reduction of 68%–73%. To illustrate, when compared with the C solution, the convergence times of the GC and GCE solutions are reduced by around 40% and 60%. This indicates that the

impact of adding 1–2 LEO satellites is more pronounced than that of the multi-GNSS combined solutions with more than 10 GNSS MEO satellites added, which demonstrates excellent performance of LEO satellites on PPP convergence.

The positioning accuracy is further assessed by calculating the RMS of positioning errors after convergence. Table 3 lists the average positioning accuracy of stations in the east, north, and up directions. It is evident that the combination of 1–2 LEO satellites mainly improves the positioning accuracy of stations in the east direction, while changes in the north and up directions are marginal. In terms of 3D positioning accuracy, the GPS PPP solution is improved from 8.9 cm to 7.2 cm and 6.9 cm with 1 and 2 LEO satellites, respectively. In the

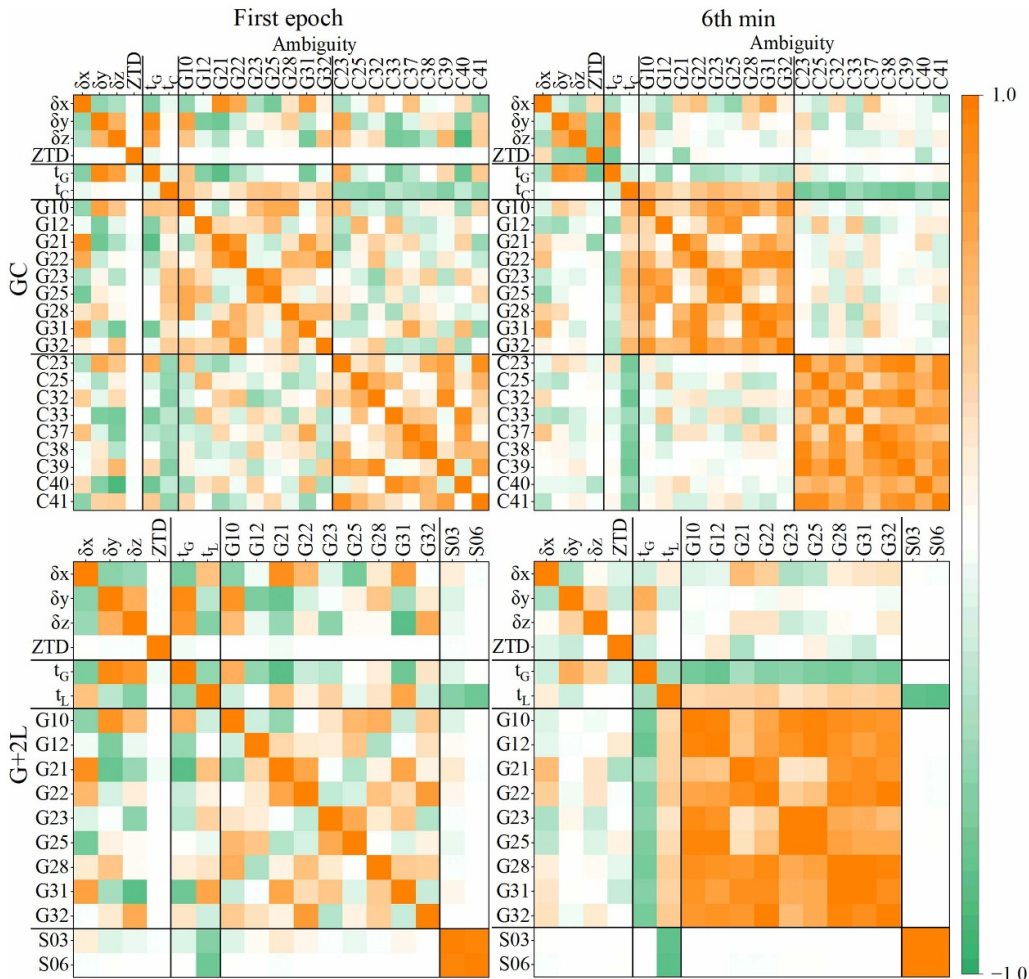


Figure 10. Correlations between parameters at the first epoch and the 6th min of the GC and G + 2L PPP at the station DG10.

Table 2. Convergence time and improvement percentage for different combinations of GNSS PPP solutions with the augmentation of 1 and 2 LEO satellites.

System	W/O LEO (min)	With 1 LEO			With 2 LEO	
		Convergence time (min)	Improvement percentage		Convergence time (min)	Improvement percentage
G	22.1	10.1	54%		7.0	68%
C	27.3	11.3	59%		7.3	73%
GC	16.2	7.6	53%		4.8	70%
GCE	10.8	4.4	60%		3.2	70%

case of the BDS-3 PPP solution, the C + 1L does not result in a significant change in 3D positioning accuracy, but the accuracy is enhanced from 8.1 cm to 6.9 cm for C + 2L solution. For the dual GNSS system, GC + 1L and GC + 2L reduce the 3D RMS error from 7.2 cm to 6.3 cm and 5.9 cm compared with the GC solution. The GCE achieves an optimal 3D positioning accuracy of 6.7 cm in the GNSS-only solutions, and this can be further improved to 5.6 cm by adding 1–2 satellites. In general, the introduction of 1–2 LEO satellites can enhance PPP 3D positioning accuracy by 1–2 cm with an improvement of 10%–20%. It should be noted that the LEO satellites are involved in PPP processing only in the first 10 min, and the accuracy statistics are from PPP convergence time

up to 1 h. With more LEO navigation satellites available in the future, the contributions of LEO observations will last for much longer time, and PPP accuracy will be further improved.

4.3. Correlation analysis between parameters

According to the above experimental results, the improvement in PPP convergence speed brought by adding 2 LEO satellites to a single GNSS system is significantly better than adding another GNSS system with 7–12 MEO satellites. To explore the mechanism of LEO augmented GNSS PPP rapid convergence, the variations of the correlations between the parameters in the PPP convergence process are analyzed,

Table 3. Average positioning accuracy in the east, north, up, and 3D directions of each PPP solution without LEO, with 1 and 2 LEO satellites.

System	Direction	W/O LEO (cm)	With 1 LEO (cm)	With 2 LEO (cm)
G	East	4.7	2.5	2.2
	North	2.2	2.1	2.1
	Up	7.2	6.4	6.2
	3D	8.9	7.2	6.9
C	East	4.7	1.7	2.7
	North	1.8	2.0	2.5
	Up	6.3	7.6	5.8
	3D	8.1	8.1	6.9
GC	East	4.4	3.1	2.5
	North	1.7	1.9	1.8
	Up	5.4	5.1	5.0
	3D	7.2	6.3	5.9
GCE	East	4.6	2.9	2.3
	North	2.2	2.2	2.2
	Up	4.4	4.2	4.5
	3D	6.7	5.6	5.6

specifically taking the GPS + BDS-3 (GC) and GPS + 2 LEO (G + 2L) PPP schemes at the station DG10 as examples. In PPP processing, the station positions (δx , δy , δz), ZTD, receiver clock offsets (t_G , t_C/t_L), and float ambiguity parameters are estimated. Figure 10 illustrates the correlation coefficients between the parameters at the first epoch and the 6th min (after 6 min) of the PPP, which are calculated from the variance–covariance matrix. The number of used GPS, BDS-3 and LEO satellites during this analysis is 9, 9, and 2, respectively. It is worth noting that the t_G in the figure denotes the GPS receiver clock offsets, and the t_C and t_L denote the ISB parameters of the BDS and CENTISPACE™ LEO systems, respectively. For comparison, the correlations for the GC PPP scheme at the 20th min, when the filtering has almost completed convergence, are plotted in figure 11.

Comparing the results in the 6th min and the first epoch, it is evident that many of the correlation coefficients between the estimated parameters for G + 2L after 6 min are either close to 0 or close to ± 1 , while the correlation coefficients of GC solution in 6th min is comparable to those of the first epoch, which suggests that the correlation variations in G + 2L are much faster than those in GC. Such results are consistent with the previous simulation study in Zheng *et al* [40]. The correlation between the GPS ambiguities and the position parameters is reduced from the first epoch to 6th min in both the GC and G + 2L PPP solutions, while the correlations are weaker in the G + 2L. After 6 min, the clock offset and ambiguity parameters are highly correlated for the same system in G + 2L, which are closer to the state after the PPP filtering has finished converging (GC PPP at 20th min) as shown in figure 11. Whereas the GC PPP has not yet reached this state at the 6th min. In addition, we observe that at the start of the PPP, the correlations between the ambiguities for the same system are higher than those of different systems, while this difference is not very noticeable. As the time comes to the 6th min, the correlation coefficients between the ambiguities for the same system are close to 1 and the correlations

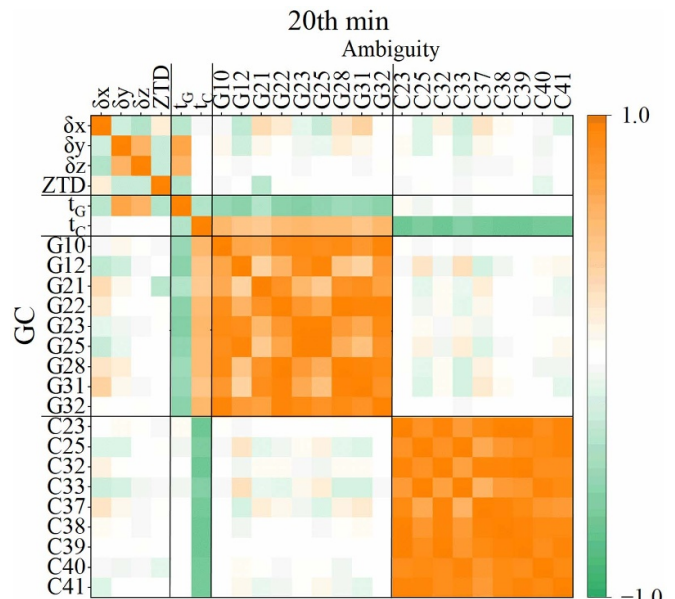


Figure 11. Correlations between parameters at the 20th min of the GC PPP at the station DG10.

between the CENTISPACE™ ambiguities and the GPS ambiguities is close to 0 in the G + 2L, which is also very similar to the case in figure 11. The analysis reveals that adding only 2 LEO satellites could lead to faster variations in correlations between parameters, compared to adding a GNSS system with 9 MEO satellites used. This demonstrates that LEO satellites are superior in accelerating the PPP convergence.

5. Conclusion

This study focuses on demonstrating the performance of LEO augmented GNSS PPP using real data from two in-orbit CENTISPACE™ experimental satellites. We first introduce

the CENTISPACE™ LEO satellites and the corresponding ground tracking data, and the characteristics of LEO navigation observations from ground stations are analyzed in terms of satellite sky plots, pseudorange noise, and multipath errors. The precise orbits of LEO satellites are determined by onboard GNSS observations, while the LEO precise clock offsets are estimated based on the observations from a ground tracking network. The RMS values of PC and LC measurement residuals for LEO downlink navigation signals are about 0.8 m and 2 cm, respectively. Then, the GNSS and LEO combined PPP is conducted to validate the performance of LEO augmented GNSS PPP in terms of convergence time and positioning accuracy.

We select three ground stations with the capability to simultaneously track dual-frequency navigation signals from GPS/BDS-3/Galileo and two LEO satellites for PPP performance analysis. The continuous tracking duration for each LEO satellite is 8–10 min, while the two LEO satellites can be observed simultaneously for about 8 min. Compared with GNSS-only PPP, the addition of 1 LEO satellite reduces the convergence time by more than 50%, while adding 2 LEO satellites can lead to a reduction of 68%–73%. In particular, the convergence time for the GPS + BDS-3 + Galileo solutions is dramatically shortened from 10.8 min to 3–5 min with only 1–2 LEO satellites involved. The correlation analysis between parameters in the PPP filtering process demonstrates that LEO satellites are superior in accelerating the PPP convergence thanks to the quick change of satellite geometry. Furthermore, the GNSS PPP positioning accuracy in 3D after convergence is enhanced by 10%–20% by introducing observations of 1–2 LEO satellites.

Although only 2 in-orbit LEO satellites are utilized to enhance the GNSS PPP, promising results are obtained and the LEO augmented GNSS performance is verified in this paper. With more LEO satellites deployed and more LEO-ground observations available in the future, it is expected that the GNSS PPP can obtain further performance improvements and rapid even instantaneous cm-level PPP convergence can be achieved.

Data availability statement

The CENTISPACE™ navigation augmentation data can be available from the corresponding author upon reasonable request and with permission of Beijing Future Navigation Tech Co., Ltd.

The data cannot be made publicly available upon publication because no suitable repository exists for hosting data in this field of study. The data that support the findings of this study are available upon reasonable request from the authors.

Acknowledgment

This work was sponsored by the National Natural Science Foundation of China (Grant Nos. 42204028, 42374030, 42030109 and 42374044), and Young Elite Scientists Sponsorship Program by CAST (2022ONRC001). The

authors acknowledged the Beijing Future Navigation Tech Co., Ltd for providing and authorizing us to process and analyze ground monitoring station data.

ORCID iDs

Xin Xie  <https://orcid.org/0000-0002-2551-2550>
Tao Geng  <https://orcid.org/0000-0001-5760-5666>

References

- [1] Zumberge J F, Heflin M B, Jefferson D C, Watkins M M and Webb F H 1997 Precise point positioning for the efficient and robust analysis of GPS data from large networks *J. Geophys. Res.* **102** 5005–17
- [2] Li X, Ge M, Dai X, Ren X, Fritzsche M, Wickert J and Schuh H 2015 Accuracy and reliability of multi-GNSS real-time precise positioning: GPS, GLONASS, BeiDou, and Galileo *J. Geod.* **89** 607–35
- [3] Ge M, Gendt G, Rothacher M, Shi C and Liu J 2008 Resolution of GPS carrier-phase ambiguities in precise point positioning (PPP) with daily observations *J. Geod.* **82** 389–99
- [4] Ge M, Doua J, Li X, Ramatschi M and Wickert J 2012 A novel real-time precise positioning service system: global precise point positioning with regional augmentation *J. Glob. Position. Syst.* **11** 2–10
- [5] Teunissen P J G, Odijk D and Zhang B 2010 PPP-RTK: results of CORS network-based PPP with integer ambiguity resolution *J. Aeronaut. Astronaut. Aviat.* **42** 223–30
- [6] Geng J, Guo J, Meng X and Gao K 2020 Speeding up PPP ambiguity resolution using triple-frequency GPS/BeiDou/Galileo/QZSS data *J. Geod.* **94** 1–15
- [7] Hein G W 2020 Status, perspectives and trends of satellite navigation *Satell. Navig.* **1** 22
- [8] Yang Y, Mao Y, Ren X, Jia X and Sun B 2024 Demand and key technology for a LEO constellation as augmentation of satellite navigation systems *Satell. Navig.* **5** 11
- [9] Enge P, Ferrell B, Bennet J, Whelan D, Gutt G and Lawrence D 2012 Orbital diversity for satellite navigation. *The 25th Int. Technical Meeting of the Satellite Division of the Institute of Navigation (ION GNSS 2012)* pp 3834–46
- [10] Reid T G, Neish A M, Walter T F and Enge P K 2016 Leveraging commercial broadband LEO constellations for navigation *The 29th Int. Technical Meeting of the Satellite Division of the Institute of Navigation (ION GNSS 2016) (Portland, Oregon, September 2016)* pp 2300–14
- [11] Joerger M, Gratton L, Pervan B and Cohen C E 2010 Analysis of iridium-augmented GPS for floating carrier phase positioning *Navigation* **57** 137–60
- [12] Yang Y X 2016 Concepts of comprehensive PNT and related key technologies *Acta Geod. Cartogr. Sin.* **45** 505–10
- [13] Yang Y, Ren X, Jia X and Sun B 2023 Development trends of the national secure PNT system based on BDS *Sci. China Earth Sci.* **66** 1–10
- [14] ESA 2024 ESA kicks off two new navigation missions (available at: www.esa.int/Applications/Satellite_navigation/ESA_kicks_off_two_new_navigation_missions)
- [15] Ge H, Li B, Nie L, Ge M and Schuh H 2020 LEO constellation optimization for LEO enhanced global navigation satellite system (LEGNSS) *Adv. Space Res.* **66** 520–32
- [16] Ma F, Zhang X, Li X, Chen J, Guo F, Hu J and Pan L 2020 Hybrid constellation design using a genetic algorithm for a LEO-based navigation augmentation system *GPS Solut.* **24** 62

- [17] Ferre R M, Praks J and Seco-Granados G 2022 A feasibility study for signal-in-space design for LEO-PNT solutions with miniaturized satellites *IEEE J. Miniaturization Air Space Syst.* **3** 171–83
- [18] Li B, Ge H, Ge M, Nie L, Shen Y and Schuh H 2019 LEO enhanced global navigation satellite system (LeGNSS) for real-time precise positioning services *Adv. Space Res.* **63** 73–93
- [19] Li X, Ma F, Li X, Lv H, Bian L, Jiang Z and Zhang X 2019 LEO constellation-augmented multi-GNSS for rapid PPP convergence *J. Geod.* **93** 749–64
- [20] Xiong S, Ma F, Ren X, Chen J and Zhang X 2021 LEO constellation augmented multi-GNSS for 3D water vapor tomography *Remote Sens.* **13** 3056
- [21] Ren X, Zhang J, Chen J and Zhang X 2021 Global ionospheric modeling using multi-GNSS and upcoming LEO constellations: two methods and comparison *IEEE Trans. Geosci. Remote Sens.* **60** 1–15
- [22] Xie X, Geng T, Zhao Q, Liu X, Zhang Q and Liu J 2018 Design and validation of broadcast ephemeris for low Earth orbit satellites *GPS Solut.* **22** 54
- [23] Meng L, Chen J, Wang J and Zhang Y 2021 Broadcast ephemerides for LEO augmentation satellites based on nonsingular elements *GPS Solut.* **25** 129
- [24] Li M, Xu T, Guan M, Gao F and Jiang N 2022 LEO-constellation-augmented multi-GNSS real-time PPP for rapid reconvergence in harsh environments *GPS Solut.* **26** 1–12
- [25] Ge H, Li B, Ge M, Zang N, Nie L, Shen Y and Schuh H 2018 Initial assessment of precise point positioning with LEO enhanced global navigation satellite systems (LeGNSS) *Remote Sens.* **10** 984
- [26] Gao W, Zhang G, Liu C, Lu J, Wang W, Chen Y, Li M and Lv F 2021 Research and simulation of LEO-based navigation augmentation *Sci. Sin. Phys. Mech. Astron.* **51** 019506
- [27] Reid T G R, Chan B, Goel A, Gunning K, Manning B, Martin J, Neish A, Perkins A and Tarantino P 2020 Satellite navigation for the age of autonomy 2020 *IEEE/ION Position, Location and Navigation Symp. (PLANS)* pp 342–52
- [28] Wang L, Chen R Z, Li D R, Zhang G, Shen X and Yu B G 2018 Initial assessment of the LEO based navigation signal augmentation system from LuoJia-1A satellite *Sensors* **18** 3919
- [29] Meng Y, Bian L and Han L 2018 A global navigation augmentation system based on LEO communication constellation 2018 *European Navigation Conf. (ENC)* pp 65–71
- [30] Wu Z, Yu B, Sheng C, Zhang J, Xie S and Wu C 2022 In-flight performance analysis of the navigation augmentation payload on LEO communication satellite: a preliminary study on WT01 mission *Geo-Spat. Inf. Sci.* **25** 88–103
- [31] Li W, Yang Q, Du X, Li M, Zhao Q, Yang L, Qin Y, Chang C, Wang Y and Qin G 2024 LEO augmented precise point positioning using real observations from two CENTISPACE™ experimental satellites *GPS Solut.* **28** 44
- [32] Xu S, Yang Q, Du X, Xu X, Zhao Q, Yang L, Qin Y and Guo J 2024 Multi-GNSS precise point positioning enhanced by the real navigation signals from CENTISPACE™ LEO mission *Adv. Space Res.* **73** 4175–86
- [33] Yang L 2023 In-orbit testing results of CENTISPACE™ LEO augmentation experimental satellites *17th Meeting of the Int. Committee on Global Navigation Satellite Systems (ICG-17) (Madrid, Spain, 15–20 October 2023)*
- [34] Chen L et al 2023 Performance evaluation of centispace navigation augmentation experiment satellites *Sensors* **23** 5704
- [35] Guo J, Xu X, Zhao Q and Liu J 2015 Precise orbit determination for quad-constellation satellites at Wuhan University: strategy, result validation, and comparison *J. Geod.* **35** 1–17
- [36] Saastamoinen J 1972 Atmospheric correction for the troposphere and stratosphere in radio ranging satellites *The Use of Artificial Satellites for Geodesy (Geophysical Monograph Series vol 15)* ed S W Henriksen, A Mancini and B H Chovitz (American Geophysical Union) pp 247–51
- [37] Boehm J, Niell A, Tregoning P and Schuh H 2006 Global mapping function (GMF): a new empirical mapping function based on numerical weather model data *Geophys. Res. Lett.* **33** L07304
- [38] Wu J, Wu S, Hajj G, Bertiger W and Lichten S 1993 Effects of antenna orientation on GPS carrier phase *Manuscr. Geod.* **18** 91–98
- [39] Petit G and Luzum B 2010 2010 IERS conventions *IERS Technical Note 36 International Earth Rotation and Reference System Service (IERS)*, Frankfurt, Germany
- [40] Zheng Y, Ge H and Li B 2023 The convergence mechanism of low Earth orbit enhanced GNSS (LeGNSS) precise point positioning (PPP) *Geo-Spat. Inf. Sci.* **27** 2211–26